Supporting Information

He et al. 10.1073/pnas.1703205114

SI Materials and Methods

Molecular Biology. The QF2.0 cDNA was obtained from Chris Potter, Johns Hopkins School of Medicine, Baltimore (48). The cDNA of fly Notch was cloned from a whole-fly cDNA preparation. The cDNA of mouse Notch was obtained from Clifford Tabin, Harvard Medical School, Boston. The cDNA of worm Notch/GLP-1 was cloned from a whole-*Caenorhabditis elegans* cDNA preparation. The cDNA of GFP-binding nanobody (GBN) was synthesized by Integrated DNA Technologies (18). The destination vectors, pWALIUM10-roe, pCaspR4 hs Gateway, *Drosophila Ubiquitin* promoter (pUbi) Gateway, and pElav Gateway with an attB sequence for site-directed insertion, were from laboratory stocks.

A PCR assay was performed with the proofreading enzyme Phusion (New England Biolabs). Plasmid purification, PCR purification, and gel extraction were performed with a QIAprep Spin Miniprep Kit (QIAGEN), QIAquick PCR Purification Kit (QIAGEN), and QIAquick Gel Extraction Kits (QIAGEN), respectively. In-Fusion cloning and Gateway cloning were performed using In-Fusion HD Liquid Kits (Clontech), and BP and LR Clonase Enzyme Mixes (Thermo Fisher Scientific). All cloning experiments were verified by DNA sequencing.

Signal peptide (SP) from mouse CD8 transmembrane (TM) glycoprotein (MASPLTRFLSLNLLLLGESIILGSGEA), GBN, and QF2.0 with 3XMyc tag were amplified by PCR and assembled into pENTR vector using In-Fusion cloning. A 28-aa linker sequence (SSPRGGGASGGGSGGGGSGGGPRGLADL) was added between the GBN and synNotch sequence to provide maximal flexibility of GFP binding from any direction. To generate GBN-synNQs, different sequences of fly, mouse, and worm Notch receptors were cloned by PCR and inserted between the GBN and QF. The PEST domain of fly Notch (amino acids 2,593–2,703) was inserted between the QF and 3XMyc tag. The synNQ (FNQ9) in the pENTR vector was subcloned into pCaspR4 hs and pUbi Gateway destination vectors. To generate the *FRT > synNQ.Stop. FRT > mcd8GFPSer* construct, synNQ with Hsp70 polyadenylation signal flanked by the FRT sequence (GAAGTTCCTATACTTTCTAGAGAATAGGAACTTC) was amplified by PCR and inserted-before the kozak sequence (AAA) of the GFP-mcd8-Ser ligand in the pENTR vector. The resulting construct was subsequently recombined into the pUbi-GWattB and pElav-GWattB destination vectors.

For the generation of different GFP-mcd8 ligands, SP of mcd8, EGFP, and the coding sequence of mcd8 (amino acids 33–222) was amplified by PCR and assembled in the pENTR vector using In-Fusion assembly. A 22-aa flexible linker (SRSGGGASGGGSGGGGSGGGRS) was inserted between the GFP and mcd8. Endocytosis signals of Delta, Serrate, or low-density lipoprotein were inserted at the C-terminal of mcd8. GPI anchoring signal (SSNKSISVYRDKLVKCGGISLLVQNTSWMLLLLLSLSLLQALDFISL) from Thy-1 was used to replace the TM domain of mcd8 (amino acids 195–222). Protein dimerization signals from the TM domain of Neuropilin-1 (NRP1; ILITIIAMSALGVLLGAVCGVVLYRKR) or Discoidin domain receptor tyrosine kinase 1 (DDR1; AILIGCLVAIILLLLLIIALMLW) were used to replace the TM domain of mcd8.

A shRNA against *Lgl* (sequence: CACGAAGATGGTTCTGTTAAA) was generated as previously reported and inserted into pQUAS Gateway expression vector (49). Transgenic flies were generated by BestGene, Inc., using phiC31 site-directed insertion.

Cell Culture Experiments. The pET-6×HisGFP was transformed into BL21 bacteria and induced by 0.5 mM isopropyl-β-D-thiogalactopyranoside for 12 h. His-tagged GFP was purified as previously described using Ni-NTA agarose beads (Thermo Fisher Scientific) (50). The purified GFP was dialyzed against PBS buffer and concentrated to 2.0 mg/mL using a 3-kDa Amicon Ultra-15 Centrifugal Filter Unit.

Drosophila S2R-positive cells were grown in Schneider's *Drosophila* media (Gibco) supplemented with 10% FBS and 0.5% penicillin/streptomycin. Cells were transfected using the Effectene transfection reagent (QIAGEN). To test the efficiency of the synthetic Notch system, cells in one well of a 12-well plate were transfected with DNA mixture that contains 0.01 μg of synNQ in pUbi vector and 0.19 μg of pQUAS-luciferase (for signal-receiving cells) or 0.2 μg of pUbi-GFP ligand (for signal-sending cells). After 2 d of transfection, the signal-sending and signal-receiving cells were washed twice in fresh culture medium, suspended, and mixed together in a 1:1 ratio. The cell mixture was cultured for one additional day before testing for luciferase activity. For the ligand and receptor cotransfection experiment, 0.01 μg of synNQs in pUbi vector, 0.01 μg of pUbi-GFP ligand, and 0.18 μg of pQUAS-luciferase were transfected into S2R-positive cells (a mixture containing 0.01 μg of empty vector, instead of pUbi-GFP ligand, was used as a control). A luciferase assay was performed using the Steady-Glo Luciferase Assay Kit (Promega), and bioluminescent signal was collected on a SpectraMax Paradigm Multi-Mode Microplate Reader.

***Drosophila* Stocks and Genetics.** The following strains were obtained from the Bloomington Drosophila Stock Center: *Hemese-Gal4* (8699); *Hemese-Gal4*, *UAS-nlsGFP* (8700); *ptc-Gal4* (2017); *R28H05-Gal4* (49472); *UAS-Flp-PEST* (55807); *QUAS-tdTomato3XHA/CyO* (30043); and *hs-Flp*, *UAS-mcd8GFP*, *QUAS-tdTomato3XHA* (30118). The *btl-Gal4* (109128) was from the Kyoto Stock Center. The *slit-Gal4/CyO* was from C. Klambdt, University of Münster, Münster, Germany. *QUAS-Lgl^{RNAi}*, *Myo1A-Gal4*, *Dpp-Gal4*, *HmlΔ-Gal4*, and *dMef-Gal4* were from laboratory stocks.

UAS-GFPmcd8Ser was inserted on the second chromosome (attP40), and *hs-synNQ*, *hs-synNQ-PEST*, *Ubi-synNQ*, *Ubi-FRT > synNQ.Stop.FRT > GFPmcd8Ser*, *Elav-FRT > synNQ.Stop.FRT > GFPmcd8Ser*, and *QUAS-Lgl^{RNAi}* were inserted on third chromosome (attP2).

Immunohistochemistry. Different *Drosophila* tissues were dissected and fixed in 4% formaldehyde, blocked by 2% BSA, incubated with a first antibody at 4 °C overnight, washed and incubated with a second antibody for 1 h at room temperature, and finally washed and mounted in Vectashield with DAPI (Vector Laboratories). The following primary antibodies were used: mouse anti–c-Myc antibody (9E10; Santa Cruz Biotechnology), chicken anti-GFP (ab13970; Abcam), mouse anti-HA (ab18181; Abcam), and mouse anti-Repo (DSHB). Secondary antibodies were goat anti-chicken Alexa 488, goat anti-mouse Alexa 488, Alexa 555, and Alexa 647 (used at 1:500; Molecular Probes).

Microscopy and Image Processing. All images were acquired on Zeiss LSM 780 confocal microscope at 405 nm (for DAPI), 488 nm (for EGFP), 561 nm (for tdTomato), and 633 nm (for Alexa 647). Objectives used were Plan-Neofluar 10×/0.30 lens, Plan-Neofluar 25×/oil 0.8-N.A. lens, and Plan-Apochromat 63× DIC (differential interference contrast) 1.4-N.A. lens. In all micrographs, blue staining shows the nuclear marker DAPI. All images were adjusted and assembled in NIH ImageJ.

The genotypes used in each figure are as follows:

QUAS-tdTomato3XHA; UAS-GFPmcd8Ser/ptc-Gal4; pUbi-synNQ (Fig. 1*D*)

UAS-Flp-PEST; QUAS-tdTomato3XHA/ptc-Gal4; pUbi-FRT > synNQ.Stop.FRT > GFPmcd8Ser (Fig. 2*C*)

UAS-Flp-PEST/tub-Gal80ts; QUAS-tdTomato3XHA/ptc-Gal4; pUbi-FRT > synNQ.Stop.FRT > GFPmcd8Ser (Fig. 2*F*)

hs-Flp, QUAS-tdTomato3XHA; pUbi-FRT > synNQ.Stop.FRT > GFPmcd8Ser (Fig. 3)

UAS-Flp-PEST; QUAS-tdTomato3XHA/btl-Gal4; pUbi-FRT > synNQ.Stop.FRT > GFPmcd8Ser (Fig. 4 *A–D*)

UAS-Flp-PEST; QUAS-tdTomato3XHA/slit-Gal4; pUbi-FRT > synNQ.Stop.FRT > GFPmcd8Ser (Fig. 4 *E–G*)

UAS-Flp-PEST; QUAS-tdTomato3XHA; pUbi-FRT > synNQ. Stop.FRT > GFPmcd8Ser/He-Gal4 (Fig. 4*H*)

UAS-Flp-PEST; QUAS-tdTomato3XHA; pUbi-FRT > synNQ. Stop.FRT > GFPmcd8Ser/Elav-Gal4 (Fig. 4*I*)

UAS-Flp-PEST/tubGal80ts; QUAS-tdTomato3XHA; Elav-FRT > synNQ.Stop.FRT > GFPmcd8Ser/R28H05-Gal4 (Fig. 4 *J* and *K*)

hs-Flp, QUAS-tdTomato3XHA; pUbi-FRT > synNQ.Stop.FRT > GFPmcd8Ser and *hs-Flp, QUAS-tdTomato3XHA; pUbi-FRT > synNQ.Stop.FRT > GFPmcd8Ser/QUAS-Lgl^{RNAi}* (Fig. 5)

hs-synNQ (Fig. S2*A*)

UAS-tdTomato3XHA; hs-synNQ (Fig. S2*B*)

hs-Flp, QUAS-tdTomato3XHA; pUbi-FRT > synNQ.Stop.FRT > GFPmcd8Ser (Fig. S3)

UAS-Flp-PEST; QUAS-tdTomato3XHA/ptc-Gal4; pUbi-FRT > synNQ.Stop.FRT > GFPmcd8Ser (Fig. S4*A*)

UAS-Flp-PEST; QUAS-tdTomato3XHA; pUbi-FRT > synNQ. Stop.FRT > GFPmcd8Ser/dMef-Gal4 (Fig. S5 A–*C*)

UAS-Flp-PEST; QUAS-tdTomato3XHA/esg-Gal4; pUbi-FRT > synNQ.Stop.FRT > GFPmcd8Ser (Fig. S5*D*)

UAS-Flp-PEST; QUAS-tdTomato3XHA; pUbi-FRT > synNQ. Stop.FRT > GFPmcd8Ser/He > Flp (Fig. S6*A*)

UAS-Flp-PEST; QUAS-tdTomato3XHA; pUbi-FRT > synNQ. Stop.FRT > GFPmcd8Ser/ He > Flp, UAS-nlsGFP (Fig. S6 *B* and *C*)

UAS-Flp-PEST; QUAS-tdTomato3XHA; pUbi-FRT > synNQ. Stop.FRT > GFPmcd8Ser/HmlΔ>Flp, UAS-nlsGFP (Fig. S6*D*)

UAS-Flp-PEST; QUAS-tdTomato3XHA; pUbi-FRT > synNQ. Stop.FRT > GFPmcd8Ser/Elav-Gal4 (Fig. S7)

UAS-Flp-PEST; QUAS-tdTomato3XHA/dpp-Gal4; pUbi-FRT > synNQ.Stop.FRT > GFPmcd8Ser (Fig. S8*A*)

UAS-Flp-PEST/ tubGal80ts; QUAS-tdTomato3XHA/Gr21a-Gal4; pElav-FRT > synNQ.Stop.FRT > GFPmcd8Ser (Fig. S8*B*)

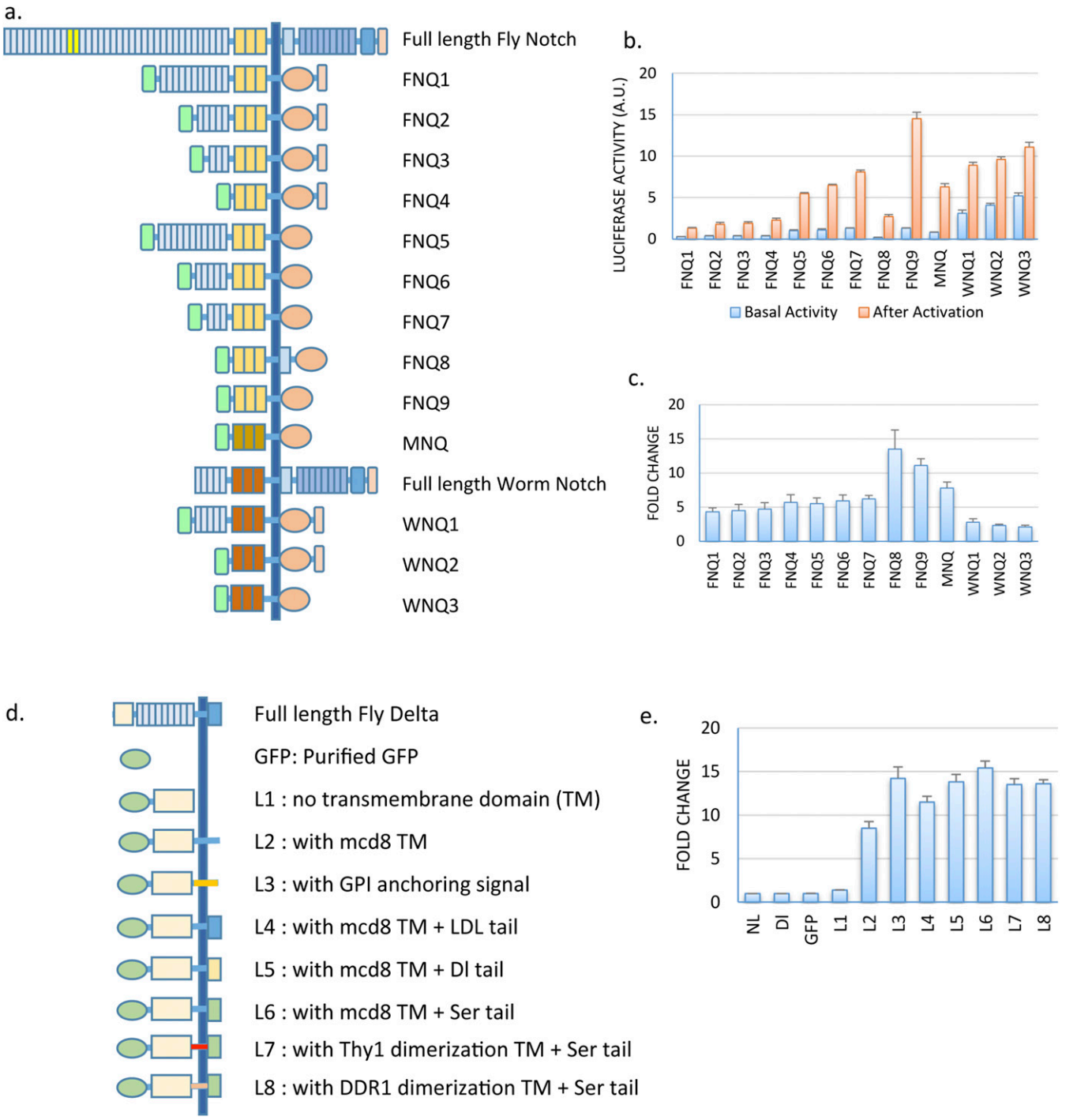

Fig. S1. In vitro optimization of synNQs and ligands in cultured cells. (*A*) Schematic illustrations of different synNQs tested in fly tissue culture. FN, fly Notch; MN, mouse Notch; WN, worm Notch. A series of deletions of EGF repeats was generated. The C-terminal end of the Notch receptor contains a PEST [proline (P), glutamic acid (E), serine (S) and threonine (T)-rich] degradation domain that may negatively regulate the stability of the Notch intracellular domain. The PEST domain may work as a mechanism to reduce the undesirable background activation of Notch by controlled proteolysis. Including a small portion of the endogenous Notch cytoplasmic domain (FNQ8) significantly reduced both the background and ligand-triggered activity, which is probably due to the presence of a myristoylation signal in the region. (*B*) Test of the activation efficiency of the activity different synNQs using a luciferase assay. All receptors were activated by mixing with cells expressing the GFP-mcd8-LDL ligand. QUAS-luciferase was used as a reporter for the receptor activation. A.U., arbitrary unit. (*C*) Fold changes of receptor activation before and after activation. FNQ9 was used for further in vivo studies and termed synNQ. (*D*) Schematic illustration of different GFP ligands tested in tissue culture. The PDZ-binding motif for Delta or Serrate (Ser) ligands was added to the tail of the artificial ligand, because the cytoplasmic tail of the ligands undergoes ubiquitination, which further promotes endocytosis and generates the pulling force. Adding the cytoplasmic tail or endocytotic signal from LDL to the artificial mcd8 ligand can increase the response of the synNQ up to 50–90%. The GPI anchoring signal and dimerization of transmembrane domains were used to cluster the acritical ligand to test if changes in local ligand concentration affect the activation efficiency. (*E*) Fold changes of luciferase activities using different GFP ligands. FNQ9 (synNQ) was used for the assay. The error bar indicates SEM. DI, Delta; NL, no ligand.

a. Expression *hs::synNQ* in larval wing disc

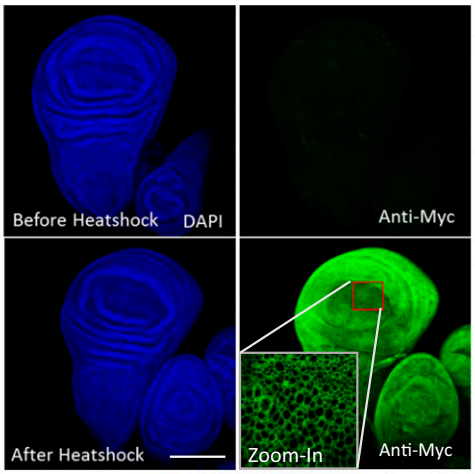

b. Spontaneous activation of *hs::synNQ*, QF activity was reported using *QUAST-tdTomato*

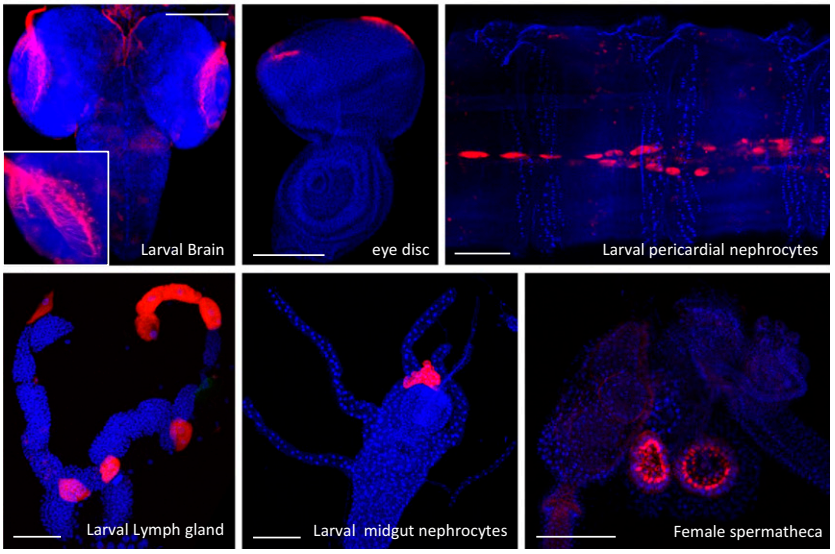

Fig. S2. In vivo expression and spontaneous activation of the synNQ. (*A*) Expression of *hs-synNQ-Myc* in the third-instar larval wing disk. After hs at 37 °C for 60 min, strong synNQ expression was detected in essentially all fly tissues after 1 d (an example of a wing disk is shown here). A high-magnification image showing that the receptor localizes correctly to the plasma membrane is included. (*B*) *hs-synNQ, QUAS-tdTomato* animals were used to test the ligand-independent activation of synNQ. Larvae or adult flies were heat-shocked for at 37 °C for 60 min 1 d before dissection. Different tissues were tested, including larval CNS, imaginal disks, midgut, fat body, and lymph gland as well as adult brain, midgut, ovary, and testis. Receptors were activated in posterior photoreceptors in eye disks that project axons into the larval optic lobe, pericardial nephrocytes associated with larval heart and lymph gland, nephrocytes associated with larval midgut proventriculus, and large secretory cells in the female spermatheca. No signal is detected in *QUAS-tdTomato*-only samples. (Scale bars: 100 μm.)

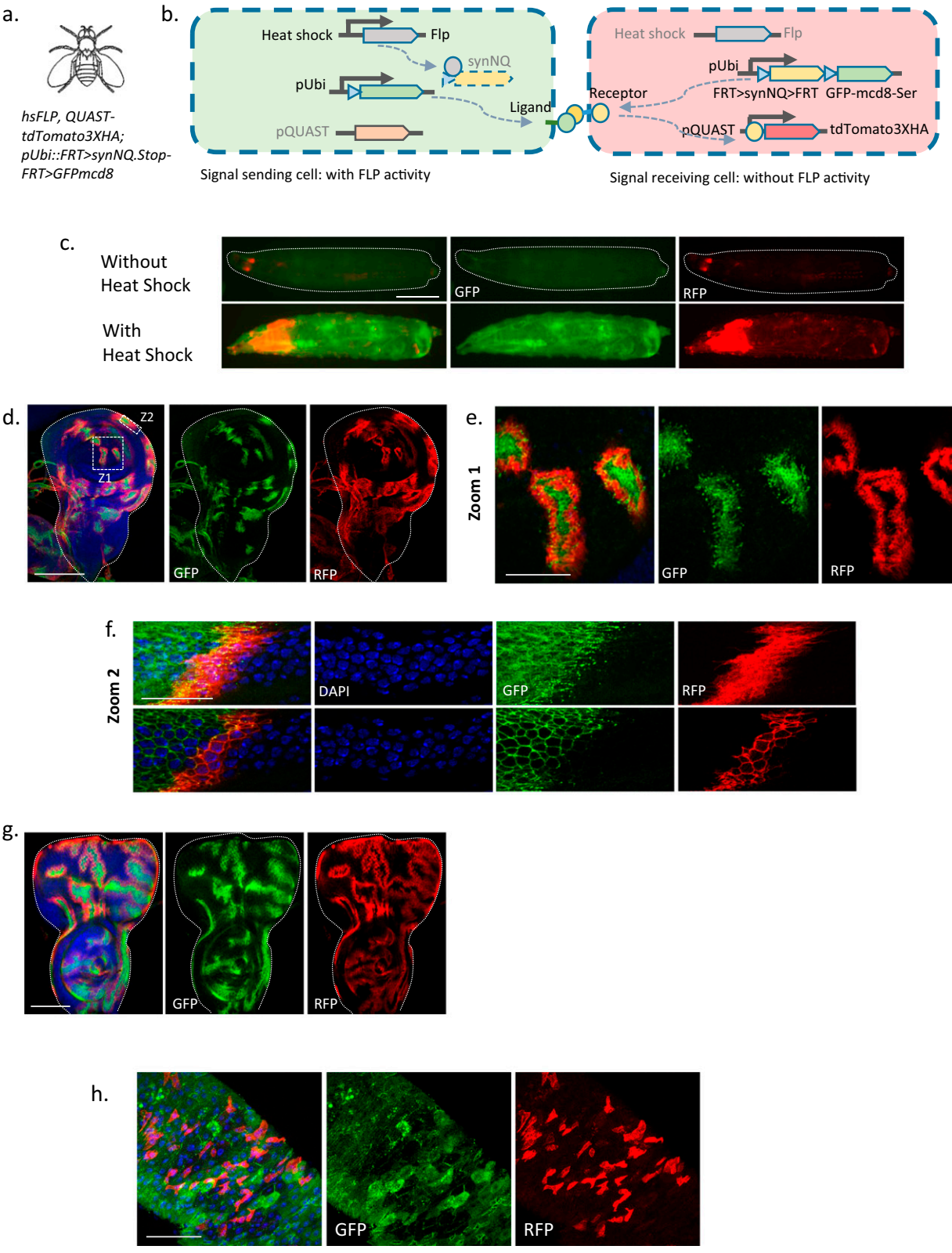

Fig. S3. Activation of synNQ by randomly generated ligand-positive cells. (*A*) Genotype of flies used in the experiments. (*B*) Schematic illustration of synNQ FLP-out system using FLP driven by hs promoter (*hsFlp*). (*C*) Larvae were heat-shocked at 37 °C for 30 min and tested for receptor activity after 5 d. Controls were kept at 25 °C without hs. (*D*–*G*) Activation of the synNQ receptor surrounding the GFP-ligand–expressing clones in wing and eye disks. Cytoneme-like membrane structures were observed in cells expressing the GFP ligand but not in the membrane-tethered tdTomato cells. (*H*) Activation of synNQ in the adult midgut. (Scale bars: *C*, 500 μm; *D*, *G*, and *H*, 100 μm; *E* and *F*, 50 μm.)

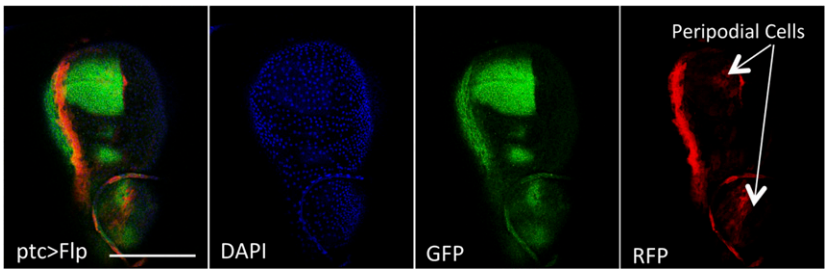

Fig. S4. In vivo activation of synNQ by *ptc-Gal4*. A projection of the z-section of peripodial cells is shown. Activation of synNQ in squamous centripetal cells is indicated by arrows. (Scale bar: 100 μm.)

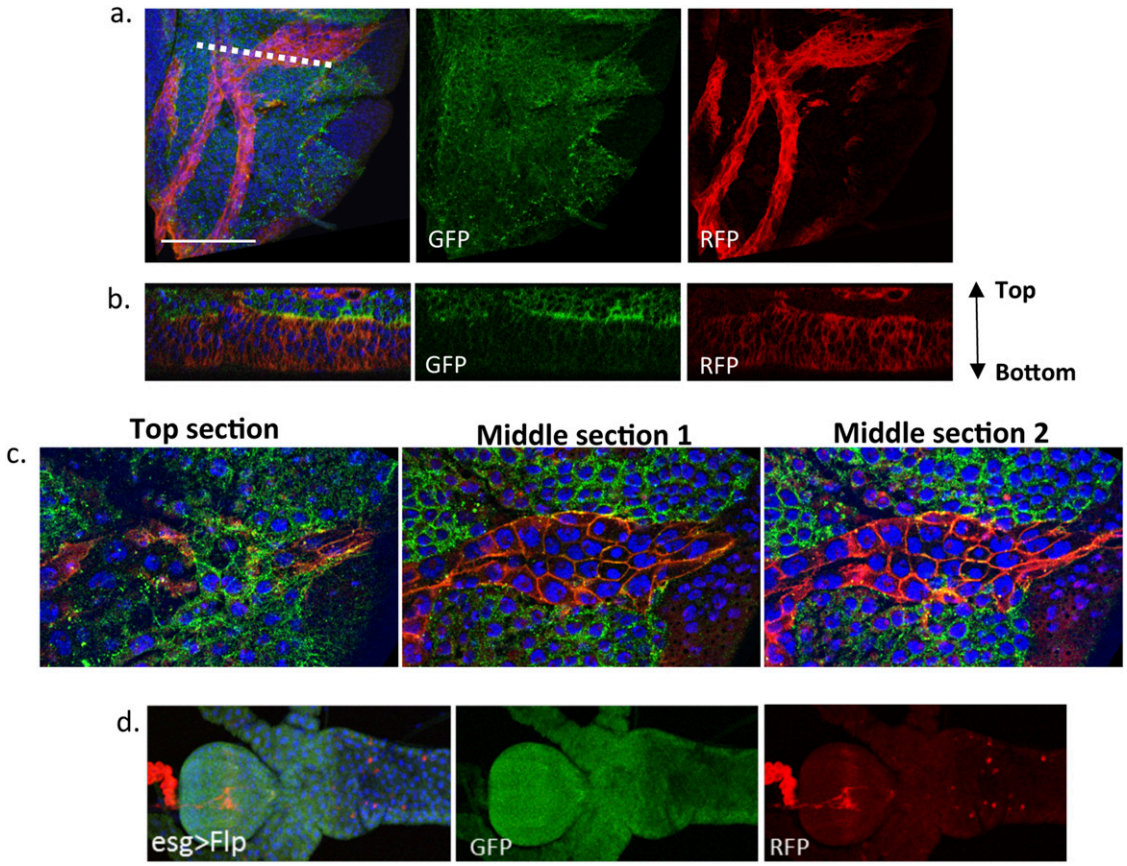

Fig. S5. In vivo activation of synNQ by *dMef-Gal4*. (*A*) Activation of synNQ in the air sac and trachea cells by myoblast cells in the wing disk. The dotted line indicates the position of Z-section shown in *B*. (*B*) GFP ligand expressed in disk-associated myoblast activates synNQ in both trachea cells and underlying wing disk epithelium. (*C*) Fibroblast-like cells associated with the tracheal tissue are GFP-positive myoblast cells. Images (from left to right) are different focal planes taken from the top section to the middle section. (*D*) Expression of GFP in larval midgut epithelium does not activate synNQ in the neurons. (Scale bar: 50 μm.)

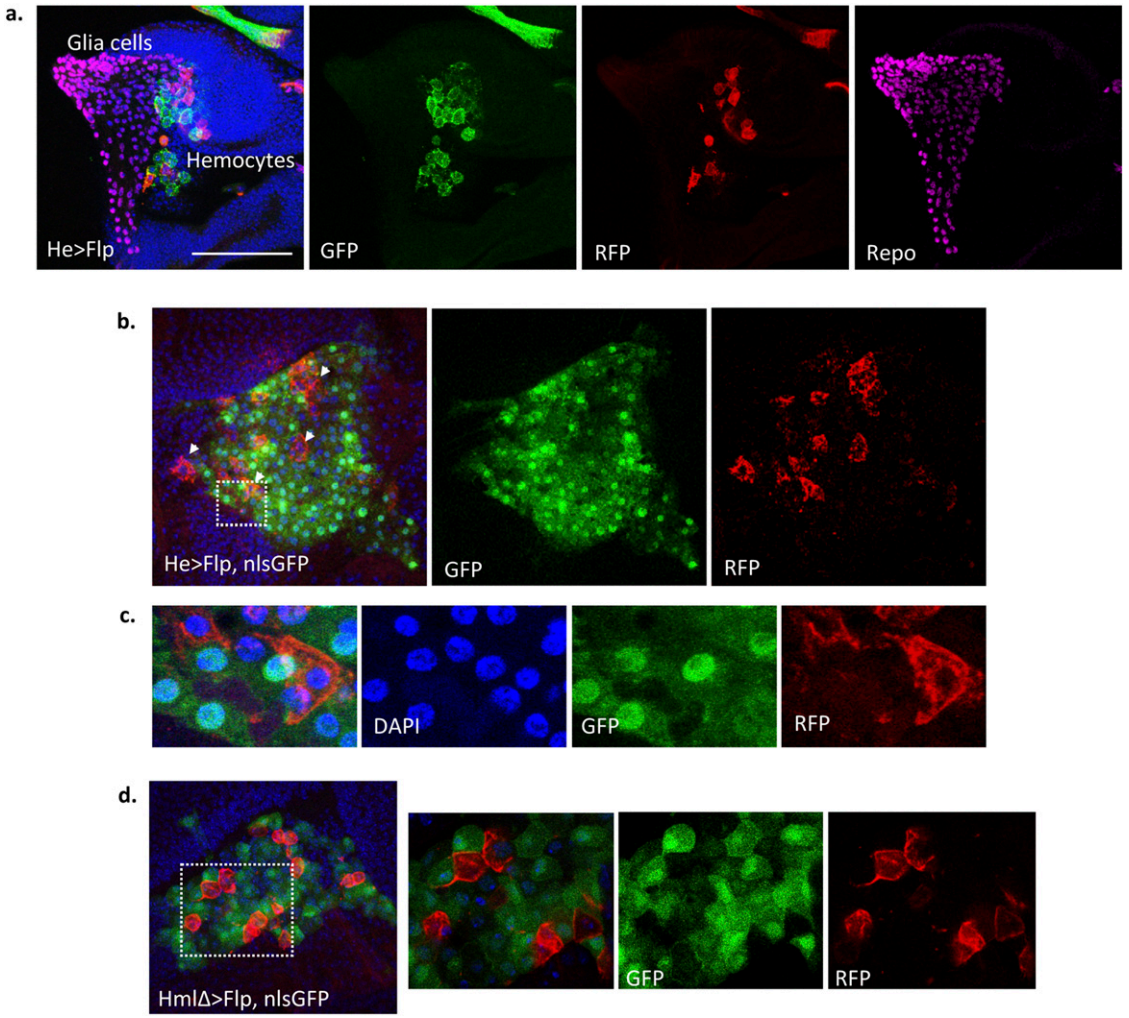

Fig. S6. In vivo activation of synNQ in eye disk-associated hemocytes. (*A*) Glia cells that migrate into the eye imaginal disk are stained by anti-Repo antibody. (*B* and *C*) *He-Gal4*, *UAS-nlsGFP* is used to activate synNQ in eye disk-associated hemocytes. Cells with synNQ activity are negative for nlsGFP. The dotted box (B) indicates the position of zoomed-in image (C). The arrowheads (B) indicate cells that are *He* negative and synNQ positive. (*D*) *HmlΔ-Gal4*, *UAS-nlsGFP* is used to activate synNQ in eye disk-associated hemocytes. The dotted box indicates the position of the zoomed-in image on the right. (Scale bar: 50 μm.)

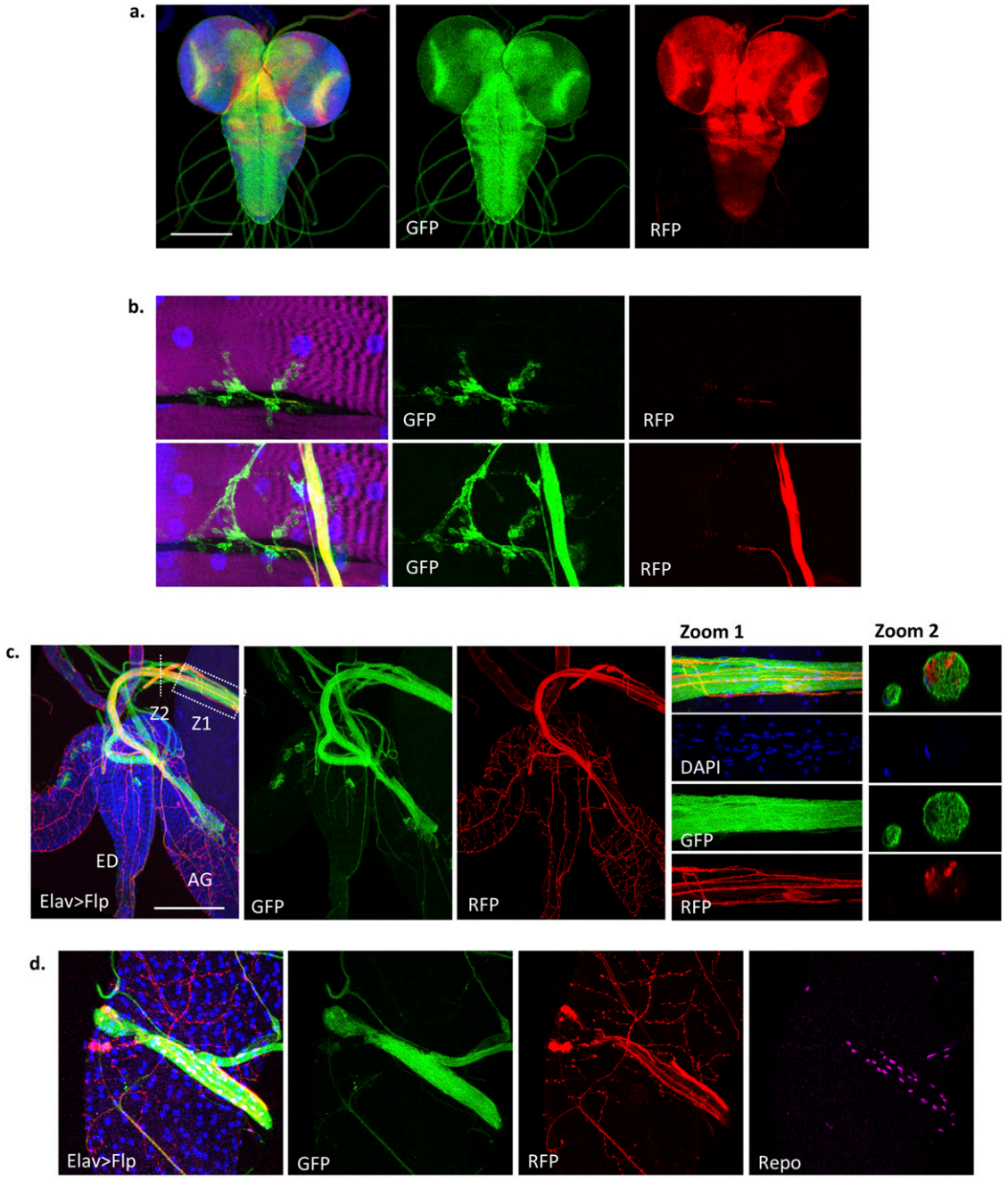

Fig. S7. In vivo activation of synNQ by Elav::Gal4. (*A*) SynNQ activity is activated using pan-neuron *Elav-Gal4* in the larval CNS. (*B*) Expression of GFP ligand in larval motor neurons and activation of synNQ in the associated glia cells. A projection of different depths of the z-stack is shown: surface (*Top*) and entire z-stack (*Bottom*). (*C*) Activation of synNQ in the male reproductive organ. The GFP ligand is expressed in the ensheathing glia cells (Repo-positive). A zoom-in view (zoom 1) and z-section (zoom 2) of the neuron projection are shown. The dotted line and dotted box indicate the positions of zoomed-in images in columns zoom 1 and zoom 2, respectively. (*D*) Magnification of the motor neurons innervating the accessary gland. AG, accessary gland; ED, ejaculatory duct. (Scale bars: *A*, 100 μm; *C*, 500 μm.)

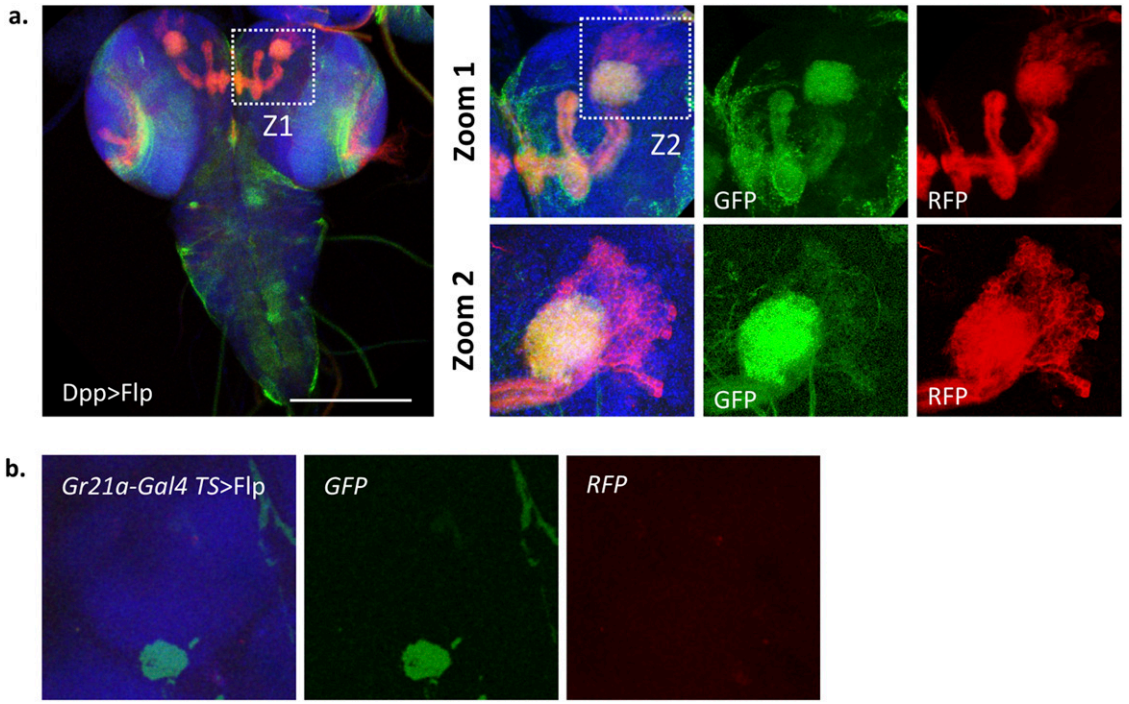

Fig. S8. In vivo activation of synNQ in the mushroom body (MB) of the larval brain. (*A*, *Left*) Activation of synNQ with *Dpp-Gal4* in the larval MB. (*A*, *Right*) Receptor activation in the MB is magnified (regions are indicated by white boxes). SynNQ is activated in cells closely associated with the GFP-positive cell cluster. However, no significant neuron in or out of the cluster was observed. (*B*) No significant synNQ activation was observed by *Gr21a-Gal4* in the fly brain olfactory lobe. Z1, zoom 1; Z2, zoom 2. (Scale bar: 100 μm.)

Other Supporting Information Files

Dataset S1 (PDF)